

Electronic band structure of magnesium and calcium oxides

N. Daude, C. Jouanin, and C. Gout

Centre d'Etudes d'Electronique des Solides, associé au Centre National de la Recherche Scientifique, Université des Sciences et Techniques du Languedoc, Place E. Bataillon, 34060 Montpellier, France

(Received 5 May 1975)

The electronic band structures of magnesium and calcium oxides are calculated by a combined tight-binding and pseudopotential method; we show the possibility of having two excitonic transitions in CaO and one in MgO, which is in agreement with experimental results. We also propose an interpretation of the other experimental results.

I. INTRODUCTION

Reflectance and thermorefectance spectra in magnesium and calcium oxides have helped to identify some electronic transitions, from 5 eV to about 35 eV.¹⁻⁵ Study of the temperature variation of the spectra reveals only one excitonic transition in^{2,3} MgO (at about 7.7 eV), and two in⁴ CaO (at about 7 and 11.4 eV). This is a result similar to that obtained with alkali halides where the conduction *d* bands play an important role. For example, the experimental curves show one excitonic peak in NaCl whereas there were two in KCl.⁶ It is widely accepted now that the second excitonic peak which appears in KCl is associated with the *d*-band edge at *X*.⁷

We present in this article calculations of the band structure for MgO and CaO. Our results show in particular that the entire *d* conduction bands are situated above the *s* bands in the case of MgO, whereas for CaO, at the point *X* the *d* states are below the *s* states, which creates a situation analogous, for example, to that for KCl. The calculated transitions are in good agreement with the experimental transitions.

MgO and CaO have both insulating properties such as a wide optical gap (~7 eV in CaO and ~8 eV in MgO) and semiconducting properties such as a wide valence band (~8.5 eV for the two oxides) and a large dielectric constant (9.8 for MgO and 11.8 for CaO). For the calculation of the electronic band structure we have used a mixed linear combination of atomic orbitals-pseudopotential method which has been shown to be both convenient and efficient in the study of ionic crystals.⁸⁻¹⁰

The filled bands have been calculated in the tight-binding scheme. The evolution of those bands in relation to the number of neighbors and with the use of several models of exchange potential, have been studied. In order to obtain a good convergence it is necessary to take into account the sixth neighbors for negative-negative ion inter-

actions, while the positive-positive ion interactions and negative-positive ones can be omitted from the second neighbors and on. With a Robinson-Bassani-Knox-Schrieffer (RBKS) exchange potential¹¹ the valence band of MgO is 8.52 eV wide while the experimental value is¹² 8.54 eV; for the CaO, still using an RBKS exchange potential we have obtained a width of 8.36 eV and to our knowledge there is no result to compare with.

For the calculation of the conduction states arising from O²⁻ ions we have used the analytic pseudopotential approach proposed by Bassani and Giuliano¹³ (hereafter called BG). Apart from causing a fast convergence of the calculated energy, this model contains all the essential features of the potential, like the nonlocality and different interactions for the valence and conduction states. In addition, due to the continuity of the potential, the method avoids the inevitable oscillations of the Heine-Abarenkof model.¹⁴ However the BG model overestimates the repulsive effects of the *p* core states and for this reason the *d* conduction states have too high-energy values⁸⁻¹⁰; this is why we have used a Philipps-Kleinman¹⁵ model to calculate the conduction states arising from the positive ions (Mg²⁺ and Ca²⁺) whose cores are not distorted by the crystal potential. All these calculations are described in Secs. II and III.

In Sec. IV we compare the results of the present calculation with those obtained by other authors using other approaches and we propose an interpretation of experimental results.

II. VALANCE BANDS

We shall stress only the approximations used in giving a brief outline of the tight-binding method. In this method, eigenvalues and eigenfunctions of the Hamiltonian are obtained by solving the secular equation

$$\det |H - ES| = 0, \quad (1)$$

where H and S are, respectively, the Hamiltonian and overlap matrices constructed with the basis function $\phi_{\mu\kappa}^{\vec{k}}$.

$$\phi_{\mu\kappa}^{\vec{k}} = \frac{1}{\sqrt{N}} \sum_{\vec{n}} e^{i\vec{k} \cdot (\vec{r}_{\kappa} + \vec{R}_{\vec{n}})} u_{\nu}(\vec{r} - \vec{r}_{\kappa} - \vec{R}_{\vec{n}}). \quad (2)$$

The sum is over the lattice vectors $\vec{R}_{\vec{n}}$. The wave function $u_{\nu}(\vec{r} - \vec{r}_{\kappa} - \vec{R}_{\vec{n}})$ represents the atomic orbital with quantum numbers ν centered around an atom located at $\vec{r}_{\kappa} + \vec{R}_{\vec{n}}$ and \vec{r}_{κ} specifies the position of the κ th ion in the unit cell. Thus we have to calculate the matrix elements

$$\langle \phi_{\mu\kappa}^{\vec{k}} | V(\vec{r}) | \phi_{\mu'\kappa'}^{\vec{k}} \rangle = \epsilon_{\mu} \langle \phi_{\mu\kappa}^{\vec{k}} | \phi_{\mu'\kappa'}^{\vec{k}} \rangle + \sum_{\vec{n}} e^{i\vec{k} \cdot \vec{R}_{\vec{n}}} \langle u_{\nu}(\vec{r}) | \sum_{\vec{n}''} \sum_{\kappa''} V(\vec{r} - \vec{R}_{\vec{n}''} + \vec{r}_{\kappa''}) | u_{\nu'}(\vec{r} - \vec{r}_{\kappa'} + \vec{r}_{\kappa} - \vec{R}_{\vec{n}}) \rangle. \quad (4)$$

Here ϵ_{μ} is the energy of an electron in the μ th state of the free ion; the summation inside the second integral includes all the ionic sites except when $n' = n$ and $\kappa'' = \kappa$. We decompose the crystal potential into three terms as

$$V = V_{\text{Coul}}^{\text{S.R.}} + V_{\text{Coul}}^{\text{L.R.}} + V_{\text{ex}}, \quad (5)$$

where $V_{\text{Coul}}^{\text{S.R.}}$ and $V_{\text{Coul}}^{\text{L.R.}}$ are, respectively, the short-range and the long-range Coulomb potentials and V_{ex} the exchange term. The integrals in (4) involving $V_{\text{Coul}}^{\text{L.R.}}$ can be exactly evaluated; for terms with $V_{\text{Coul}}^{\text{S.R.}}$ and V_{ex} we make a spherical average.

In order to study the evolution of the filled bands in relation to the exchange potential, we have successively assumed it to be zero, to be equal to the Slater model¹⁶ and subsequently to the RBKS model.¹¹ When V_{ex} is put to zero, we obtain valence bands whose width is too narrow while they are too large with the Slater model. With the RBKS model we obtain a valence band with a width of 8.52 eV for MgO while Fomichev *et al.*¹² by interpreting soft-x-ray emission spectra have estimated it to be 8.54 eV. For CaO we obtain 8.36 eV.

In the RBKS model, the Coulomb term of the Slater model is screened and replaced by $(e^2/r) \times e^{-k_s r}$, with $k_s = 0.82k_F(r_s^{1/2})$, where k_F is the Fermi momentum and r_s is related to the electronic density by $\rho^{-1} = \frac{4}{3}r_s^3$. Robinson *et al.*¹¹ have shown that, when the dielectric constant is > 4 , the behavior of their model is the same as if the dielectric constant was infinite; the results we obtain with MgO and CaO confirm those conclusions.

The integrals in (4) have been expressed in terms of two-center integrals¹⁷ $ss\sigma$, $sp\sigma$, $pp\sigma$ and $pp\pi$; we have used the ionic wave functions given by Clementi¹⁸ for Mg^{++} and Ca^{++} ions, and those calculated by Watson¹⁹ for the O^{--} ion; the most important interactions are those between negative ions; the negative-positive ion interactions are

$$\langle \phi_{\mu\kappa}^{\vec{k}} | O | \phi_{\nu'\kappa'}^{\vec{k}} \rangle = \sum_{\vec{n}} e^{i\vec{k} \cdot (\vec{r}_{\kappa'} + \vec{R}_{\vec{n}} - \vec{r}_{\kappa})} \times \langle u_{\nu'}(\vec{r} - \vec{r}_{\kappa} | O | u_{\nu'}(\vec{r} - \vec{r}_{\kappa'} - \vec{R}_{\vec{n}}) \rangle. \quad (3)$$

In (3), O is either a unit operator, or the Hamiltonian operator; in the first case we have two center integrals and their calculation does not present any difficulty; but in the second case, because the crystal potential is a sum of ionic potentials, it produces three center terms which are very difficult to evaluate. In the latter case we can write (3) as

weak and the positive-positive ones negligible.

We have also studied the evolution of the filled bands as we change the number of neighbors. The results show that the positive-positive ion interactions and the negative-positive ones may be omitted from the second neighbors and on. In Tables I and II we show the position of the different valence band states with different number of negative-negative ion interactions; we can see that to have a good convergence it is necessary to take into account the 6th negative-negative ion interactions. For the next band the convergence is good from the 3rd negative-negative ion interactions.

The energy bands obtained with an RBKS exchange potential are plotted in Figs. 1 and 2.

For the two oxides the maximum of the valence band occurs at the Γ_{15} level and the minimum at the L_1 level in the case of CaO but along the direction Σ for MgO. The next band coming from the 2s

TABLE I. Energy levels (in Ry) of the valence states of MgO. The notations are those of Ref. 28, with a negative ion at the origin. The number at the top of columns 2, 3, and 4, indicates the number of negative-negative ion interactions.

	4	5	6
Γ_{15}	-1.372	-1.211	-1.182
X_5'	-1.510	-1.483	-1.457
X_4'	-1.645	-1.755	-1.741
L_3	-1.060	-1.151	-1.183
L_1	-1.810	-1.754	-1.766
K_4	-1.344	-1.286	-1.244
K_1	-1.516	-1.525	-1.554
K_3	-1.634	-1.707	-1.707
W_1	-1.344	-1.317	-1.342
W_1	-1.598	-1.660	-1.678

TABLE II. Energy levels (in Ry) of the valence states of CaO. The notations are those of Ref. 28, with a negative ion at the origin. The number at the top of columns 2, 3, and 4, indicates the number of negative-negative ion interactions.

	4	5	6
Γ_{15}	-0.920	-0.903	-0.902
X'_5	-1.071	-1.067	-1.062
X'_4	-1.416	-1.434	-1.430
L_3	-0.928	-0.941	-0.946
L_1	-1.531	-1.522	-1.519
K_4	-1.026	-1.016	-1.011
K_1	-1.224	-1.225	-1.229
K_3	-1.332	-1.344	-1.344
W_1	-1.084	-1.081	-1.088
W_1	-1.356	-1.267	-1.268

electrons of the O^{--} ion has a width of about 1.8 eV for MgO and 0.7 eV for CaO. After this band the next one is that formed by the $2p$ electrons of Mg^{++} or $3p$ electrons of Ca^{++} ; those bands are practically flat. We have to note that if we neglect the exchange potential, the Ca^{++} $3p$ electrons band is above that of the O^{--} $2s$ electrons.

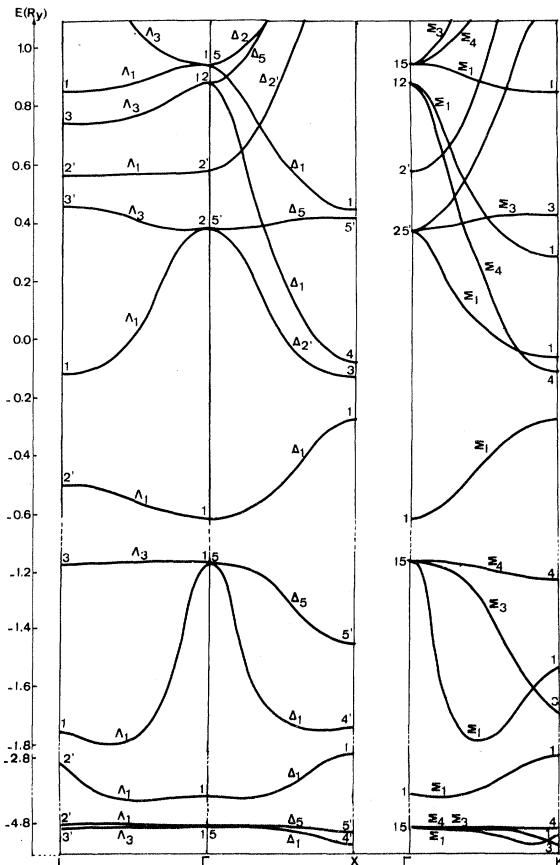


FIG. 1. Energy bands of MgO. Symmetry notations are those of Ref. 28 with the origin at an oxygen site.

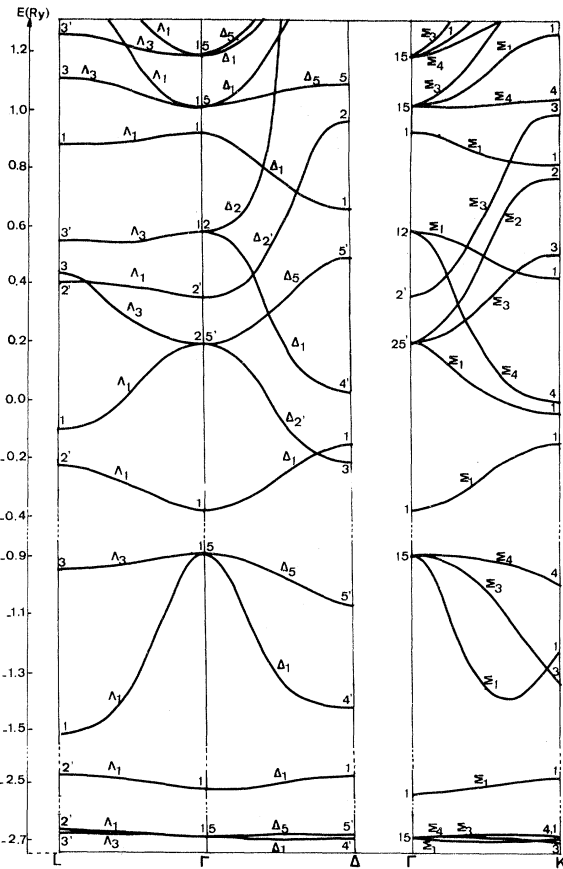


FIG. 2. Energy bands of CaO. Symmetry notations are those of Ref. 28 with the origin at an oxygen site.

III. CONDUCTION BANDS

A. Preliminary considerations

We have calculated the conduction states as those of an extra electron added to the lattice which sees the potential of the filled ionic shells.¹³ A pseudopotential should be such that it gives the same dispersion relations $E(\vec{k})$ as the true one.²⁰ In fact there are two classes of pseudopotential.

In the first type, the pseudowave equation is obtained from the true Schrödinger equation by a mathematical transformation which conserves the eigenvalues but alters the eigenfunctions. The core states are explicitly included in such a potential: for instance the Philipps-Kleinman¹³ potential is connected to the atomic potential V_a by

$$V_{ps}|\phi\rangle = V_a|\phi\rangle + \sum_c (E - E_c)\langle\psi_c|\phi|\psi_c\rangle, \quad (6)$$

where $|\phi\rangle$ is the smooth part of the wave function, E_c the energies of the core states, and the summation is extended for all the core states.

In the second type, the pseudopotential is an operator that simulates the diffusion produced by

the true potential in a particular energy region. That method presents some advantages of calculation and dispenses with the knowledge of the core states and the exact potential. Numerous models have been proposed and the most famous is that of Heine-Abarenkov¹⁴

$$V_M = \begin{cases} \sum_l A_l P_l & \text{for } r < R_c, \\ -Ze^2/r & \text{for } r > R_c, \end{cases} \quad (7)$$

where P_l is the angular momentum projection operator and A_l and R_c are adjustable parameters. Giuliano and Ruggeri²¹ have proposed the following model:

$$V_M^k = \sum_l V_l^k(r) P_l, \quad (8)$$

with

$$V_l^k(r) = -\frac{e^2 N_k e^{-\alpha_l r}}{r} - \frac{Z_\kappa e^2}{r + A_l(E)/r^2}. \quad (9)$$

Z_k and N_k are, respectively, the valence and the nuclear charge, α_l and A_l are parameters which depend on the angular momentum. We can see that this form reproduces the correct comportment of the real potential near the nucleus and at infinity and avoids the oscillations of the Heine-Abarenkov model; moreover if there are no occupied states for a given energy it is sufficient to match the relation (9) with the ionic potential. The parameters A_l and α_l are obtained from experimental data.

B. Crystal potential

In Figs. 1 and 2 we can see that the Mg^{++} and Ca^{++} bands are almost flat so that the states of the positive ions are very little distorted by the crystal potential; thus the pseudopotential has been obtained by a direct orthogonalization to the ionic orbitals following in that sense the Phillipps-Kleinman model.¹⁵ For the oxygen we have used the Giuliano and Ruggeri model already used by BG¹³ for the alkali chlorides and by Jouanin *et al.* for alkali fluorides⁹ and magnesium fluorides.¹⁰ If $l > 2$, there are no core states with such a value and α_l and A_l are obtained by matching the pseudopotential with the ionic potential; for the occupied states we took a large value of α_l because that causes a very powerful repulsive effect near the nucleus. The values of A_s and A_p are then calculated in such a way that we obtain the optical gap of MgO; the same values are adopted for CaO and as we will see in the following, the gap is in good agreement with the experimental value. In Table III we give the value of the parameters A_l and α_l .

The conduction bands are obtained by resolution of the secular equation

TABLE III. Values of the O^{--} pseudopotential parameters.

α_s	α_p	α_d	A_s	A_p	A_d
90	90	2.4	1.25	0.3	3.7

$$\det |\langle \psi_{rs}^i(\vec{k}^m) | H - E | \psi_{rs}^i(\vec{k}^n) \rangle| = 0. \quad (10)$$

$|\psi_{rs}^i(\vec{k}^n)\rangle$ is a plane-wave symmetrized combination, generated by the plane wave $|\vec{k}^n\rangle = |\vec{k}^n + \vec{K}^n\rangle$ (where \vec{K}^n is a vector of the reciprocal lattice), that belongs to the i th column of the irreducible representation Γ^i of the little group $G_{\vec{k}}$.

The matrix elements of the operator $H - E$ can be written

$$\begin{aligned} \langle \psi_{rs}^i(\vec{k}^m) | H - E | \psi_{rs}^i(\vec{k}^n) \rangle \\ = (M_s^{m/n}/t_s)^{1/2} \sum_l C_{l/ls}^{m/n} \langle \vec{k}^m | H - E | \vec{k}^n \rangle, \end{aligned} \quad (11)$$

with

$$\begin{aligned} \langle \vec{k}^m | H - E | \vec{k}^n \rangle \\ = [-\hbar^2/2m] |\vec{k}^m|^2 - E] \delta_{mm} + \langle \vec{k}^m | V_M | \vec{k}^n \rangle, \end{aligned} \quad (12)$$

and

$$\begin{aligned} \langle \vec{k}^m | V_k | \vec{k}^n \rangle = S^+(\vec{k}^m - \vec{k}^n) \langle \vec{k}^m | V^+ | \vec{k}^n \rangle \\ + S^-(\vec{k}^m - \vec{k}^n) \langle \vec{k}^m | V^- | \vec{k}^n \rangle. \end{aligned} \quad (13)$$

$S^\pm(\vec{k}^m - \vec{k}^n)$ are the structure factors for the two sorts of ions.

C. Results

Equation (10) has been solved with a basis of about 200 plane waves; the results we obtain are sketched in Figs. 1 and 2.

The behavior of the conduction bands are similar for the two oxides and can be interpreted from the free electron scheme.¹³ On the two curves the minimum of the conduction states is the Γ_1 one. The chief difference between the two oxides is the behavior of the d bands; for MgO the minimum of the d states is situated at L'_2 and that state is above the maximum of the s band; in CaO the minimum of the d states is at X_3 which is situated below some s states *but* above Γ_1 ; so, for CaO, it is possible to have excitonic transitions both at Γ and at X .

IV. DISCUSSION OF RESULTS

A. Magnesium oxide

The behavior of ϵ_2 , the imaginary part of the dielectric constant obtained from measurements of reflectivity, is similar to that of alkali halides¹⁻⁴; it presents a sharp peak at 7.7 eV, two big peaks at 10.8 and 13.2 eV, two small peaks at

TABLE IV. Comparison between the many results which are available for MgO. No one-to-one correspondence with experimental results can be established with the results of Ref. 24. The authors of Ref. 25 and 26 do not indicate the origin of the maximums at 17.4 and 19.2 eV.

Experimental results	Ref. 22	EPM Ref. 23	HFS Ref. 24	HFSC Refs. 25 and 26	Present work			
7.7 (Ref. 1) exciton			7.53					
7.77 (Ref. 2) } gap	8.15	7.77	$\Gamma_{15} \rightarrow \Gamma_1$	8.9	$\Gamma_{15} \rightarrow \Gamma_1$	7.76	$\Gamma_{15} \rightarrow \Gamma_1$	
7.83 (Ref. 3) }								
10.8 (Ref. 1)	13.3	10.885 10.893	$L_3 \rightarrow L'_2$ $\lambda_3 \rightarrow \lambda_1$	11.5	10.7	Σ, Δ, Z, U	9.38	$L_3 \rightarrow L'_2$
13.3 (Ref. 1)	13.2 13.6	13.04 13.3 16.2	$\Delta_5 \rightarrow \Delta_1$ $\Sigma_4 \rightarrow \Sigma_1$ $\lambda_3 \rightarrow \lambda_3$	14	13.2	$\left\{ \begin{array}{l} \Sigma_4 \rightarrow \Sigma_3; K_4 \rightarrow K_3 \\ W_2 \rightarrow W_3; Z_1 \rightarrow Z_3 \end{array} \right.$	13.2	$K_4 \rightarrow K_1$
16.8 (Ref. 1)	15.6	16.39 16.63	$\Sigma_4 \rightarrow \Sigma_2$ $\Delta_5 \rightarrow \Delta_1$		16.9	$\Gamma_{15} \rightarrow \Gamma'_{25}$	16.2	$\left\{ \begin{array}{l} X'_5 \rightarrow X_1 \\ K_4 \rightarrow K_1 \end{array} \right.$
	16.4							
17.3 (Ref. 1)		16.93 17.01 19.92	$X'_4 \rightarrow X_3$ $\Delta_5 \rightarrow \Delta_1$ $L_1 \rightarrow L'_3$	18	17.4		17.3	$L_1 \rightarrow L'_2$
				19	19.2		20.1	$X'_4 \rightarrow X_1$
20.5 (Ref. 1)		20.105 21.2	$K_1 \rightarrow K_1$ $W_3 \rightarrow W_3$				20.4	$K_4 \rightarrow K_1$
				22.5			21.5	$\Gamma_{15} \rightarrow \Gamma'_{25}$
24 (Ref. 4), 25 (Ref. 1)		21.704 24.755	$K_4 \rightarrow K_3$ $X_4 \rightarrow X_1$				26.1	$X_5 \rightarrow X_1$
31-40 (Ref. 4)							27	$K_4 \rightarrow K_1$
							31.5	$L_1 \rightarrow L'_2$
52-60 (Ref. 4)							37	$X_1 \rightarrow X'_4$
							58.7	$\Gamma_{15} \rightarrow \Gamma_1$
							62	$X_5 \rightarrow X_1$

16.8 and 17.3 eV, a rounded maximum at 20.5 eV, and then a broad and small structure between 23 and 24 eV; only the peak at 7.7 eV shows excitonic behavior; when the temperature drops it becomes increasingly sharp and moves towards the high energies.

The electronic structure of MgO has already been calculated by a few authors. Cohen *et al.*²² and Fong *et al.*²³ have used an empirical pseudo-potential approach (EPM); Walch and Ellis²⁴ a Hartree-Fock-Slater method (HFS) and recently, Pantelides *et al.*^{25, 26} have obtained self-consistent solutions of Hartree-Fock equations (SCHF).

For the filled bands, the different approaches give qualitatively similar results; the chief difference is the width of the valence band; it is about 3 eV wide in the HFS model, 5.5 eV with the EPM one and about 7 eV with the SCHS approach; as we have already mentioned, we obtain a width of 8.52 eV, when the experimental value is 8.54 eV.¹²

For the conduction bands, the disagreements are more important. Qualitatively our curves are similar to those obtained with the HFS calculation, but the numerical results are very different. The HFS and the EPM approaches and our results

place the minimum of the conduction states at Γ_1 and anticipate a direct gap; in the SCHF approach the minimum is at X_3 and an indirect gap is anticipated; this last approach also anticipates another minimum at L point and so an other indirect transition is possible; these indirect gaps have not been confirmed by experimental results. Only our curves and the EPM ones account for the excitonic peak at 7.7 eV, when, as is noted by their authors, this is not possible with the HFS and SCHF results.

In Table IV we give the possible interpretations of the other singularities of the experimental curves. As we can see the interpretations are different. The authors of the EPM and SCHF calculations have also calculated ϵ_2 from their band structures, and though their curves are similar, the interpretations are different; as it is noted by the authors of Refs. 25 and 26 it is possible to build a band structure from an optical spectra, but the construction is not unique.

B. Calcium oxide

Whited and Walker⁵ have obtained peaks in their reflectivity curves at 6.8, 10, 11.4, 13, 17, 27, and 35 eV. Only the peaks at 6.8 and 11.4 eV are

TABLE V. Comparison between the results which are available for CaO.

Experiment results	APW Ref. 27	Present work
6.8 (Ref. 5) exciton		
7.03 (Ref. 2) gap	9.62 $\Gamma_{15} \rightarrow X_3$	
7.08 (Ref. 3)	9.71 $\Gamma_{15} \rightarrow \Gamma_1$ 9.74 $X_{5'} \rightarrow X_3$	7.1 $\Gamma_{15} \rightarrow \Gamma_1$
10 (Ref. 5)		9.79 $L_3 \rightarrow L'_2$
11.42 (Ref. 5) exciton		11.75 $X'_5 \rightarrow X_3$
12.1 (Ref. 5)		12.88 $K_4 \rightarrow K_1$
16.9 (Ref. 5)	16.6 $2p^- \rightarrow d$	17.46 $X'_4 \rightarrow X_1$ 17.54 $L_1 \rightarrow L_2$
~27 (Ref. 5)	23 $3p^+ \rightarrow d$	23.4 $X'_5 \rightarrow X_1$
	25 $2s^- \rightarrow p$	24.98 $K_3 \rightarrow K_3$ 27.9 $L_1 \rightarrow L_3$
~35 (Ref. 5)	41 $3s^+ \rightarrow p$	31.1 $\Gamma_{15} \rightarrow \Gamma_1$
		33.7 $X'_5 \rightarrow X_3$ 39 $\Gamma_{15} \rightarrow \Gamma_{25}$

temperature dependent; through lack of band-structure calculation, the authors have assigned those peaks to the $X'_5 \rightarrow X_3$ and $X'_4 \rightarrow X_3$ excitonic transitions; the others singularities have been interpreted by comparison with MgO.

Subsequently, Mattheiss²⁷ has calculated the band structure of CaO by an augmented-plane-wave (APW) approach; those results are very different in many respects to ours, both for the valence states and the conduction ones.

The width of the valence band of the APW calculation is about 1.5 eV whereas we obtain a value of 8.36 eV. Although this parameter has not yet been measured, it can be said that it is not very different from that of MgO. The sequence of the two next bands is inverted in the two approaches. The use of two different approaches does not explain such large disagreements; atomic wave functions and a Slater exchange potential is used in the Mattheiss's calculations, whereas we use ionic wave functions and a screened Slater exchange potential; perhaps these differences are sufficient to explain the disagreements between

the two calculations; let us remark however that with a Slater exchange potential without screening, we obtain a valence bandwidth of about 10 eV and that the sequence of the next band is the same as that in the Mattheiss calculations if we use an exchange potential equal to zero.

Mattheiss remarks in addition that the interaction between the $3p$ states of the Ca atoms and the $2s$ states of O atoms is large, whereas we have already indicated that this interaction between Ca^{++} ions and O^{--} ions is insignificant. We have calculated a second time the filled bands without Ca^{++} wave functions and the results are almost the same.

The disagreement is also very considerable for the conduction bands; the APW results anticipate an indirect gap $\Gamma_{15} \rightarrow X_3$ at 9.6 eV and direct gaps at Γ and X for, respectively, 9.71 and 9.74 eV; we obtain a direct gap $\Gamma_{15} \rightarrow \Gamma_1$ at 7.1 eV. In the two calculations the minimum of the d states is at X_3 , but that state is the absolute minimum in the APW approach whereas in our calculation it is the Γ_1 state. Let us note a last difference: the Γ'_{25} state is about 3 eV above the Γ_1 state in the APW results and in ours it is 7.75 eV above.

Clearly our curves show the possibility of having two excitonic transitions at 7.1 eV ($\Gamma_{15} \rightarrow \Gamma_1$) and 11.75 eV ($X'_5 \rightarrow X_3$) and that is consistent with the experimental results. Whited and Walker estimate the gap at 7.03 eV.

In Table V we propose an interpretation of the other experimental singularities.

V. CONCLUSION

In this paper the energy bands of MgO and CaO have been calculated and the results we obtain are in good agreement with experimental results. The mixed method of calculation already used in the case of ionic crystals is also adapted for those oxides which present a few semiconducting properties such as a wide valence band and a large dielectric constant; in particular the tight-binding scheme gives good results with an RBKS exchange potential.

¹D. M. Roessler and W. C. Walker, Phys. Rev. **159**, 733 (1967).

²R. C. Whited and W. C. Walker, Phys. Rev. Lett. **22**, 1428 (1969).

³R. C. Whited, C. J. Flaten, and W. C. Walker, Solid State Commun. **13**, 1903 (1973).

⁴W. F. Hanson, E. T. Arakawa, and M. W. Williams, J. Appl. Phys. **43**, 1661 (1972).

⁵R. C. Whited and W. C. Walker, Phys. Rev. **188**, 1780 (1969).

⁶See, for instance, C. Gout and F. Pradal, J. Phys.

Chem. Solids **29**, 581 (1968); D. M. Roessler and W. C. Walker, Phys. Rev. **166**, 599 (1968).

⁷See, for instance, S. Oyama and T. Miyakawa, J. Phys. Soc. Jpn. **21**, 368 (1966); A. B. Kunz, Phys. Rev. **175**, 1147 (1968); L. J. Page and E. H. Hygh, *ibid.* **1**, 3472 (1970); M. Overhof, Phys. Status Solidi **43**, 575 (1971).

⁸C. Jouanin, thesis (Montpellier, 1974) (unpublished).

⁹C. Jouanin, J. P. Albert, and C. Gout, Nuovo Cimento B **28**, 483 (1975).

¹⁰C. Jouanin, J. P. Albert, and C. Gout, J. Phys. (Paris) (to be published).

- ¹¹J. E. Robinson, F. Bassani, R. S. Knox, and J. R. Schrieffer, *Phys. Rev. Lett.* **9**, 215 (1962).
- ¹²V. A. Fomichev, T. M. Zimkina, and I. I. Zhukova, *Fiz. Tverd. Tela* **10**, 3072 (1968) [*Sov. Phys.-Solid State* **10**, 2421 (1969)].
- ¹³F. Bassani and E. S. Giuliano, *Nuovo Cimento B* **8**, 193 (1972).
- ¹⁴V. Heine and I. V. Abarenkov, *Philos. Mag.* **9**, 451 (1964).
- ¹⁵J. C. Phillips and L. Kleinman, *Phys. Rev.* **116**, 287 (1959).
- ¹⁶J. C. Slater, *Phys. Rev.* **81**, 385 (1951).
- ¹⁷J. C. Slater and G. F. Koster, *Phys. Rev.* **94**, 1498 (1954).
- ¹⁸E. Clementi, *Tables of Atomic Functions* (I.B.M. Corp., San José, 1965)(unpublished).
- ¹⁹R. G. Watson, *Phys. Rev.* **111**, 1108 (1958).
- ²⁰J. M. Ziman, *Solid State Physics* (Academic, New York, 1971), Vol. 6.
- ²¹E. S. Giuliano and R. Ruggeri, *Nuovo Cimento B* **61**, 53 (1969).
- ²²M. L. Cohen, P. J. Lin, D. M. Roessler, and W. C. Walker, *Phys. Rev.* **155**, 992 (1967).
- ²³C. Y. Fong, W. Saslov, and M. L. Cohen, *Phys. Rev.* **168**, 992 (1968).
- ²⁴P. F. Walch and D. E. Ellis, *Phys. Rev. B* **8**, 5920 (1973).
- ²⁵S. T. Pantelides, D. J. Mickish, and A. B. Kunz, *Solid State Commun.* **15**, 203 (1974).
- ²⁶S. T. Pantelides, D. J. Mickish, and A. B. Kunz, *Phys. Rev. B* **10**, 5203 (1974).
- ²⁷L. F. Mattheiss, *Phys. Rev. B* **5**, 290 (1972); **5**, 305 (1972).
- ²⁸L. P. Bouckaert, R. Smoluchowski, and E. Wigner, *Phys. Rev.* **50**, 58 (1936).